HHS Public Access

Author manuscript

Sci Immunol. Author manuscript; available in PMC 2019 August 03.

Published in final edited form as:

Sci Immunol. 2018 August 03; 3(26): . doi:10.1126/sciimmunol.aao4747.

Neutrophil cytoplasts induce Th17 differentiation and skew inflammation toward neutrophilia in severe asthma

Nandini Krishnamoorthy[1,¶], **David N. Douda**[1,¶], **Thayse R. Brüggemann**[1], **Isabell Ricklefs**[1], **Melody G. Duvall**[1], **Raja-Elie E. Abdulnour**[1], **Kimberly Martinod**[2], **Luciana Tavares**[1], **Xiao Wang**[3], **Manuela Cernadas**[1], **Elliot Israel**[1], **David T. Mauger**[4], **Eugene R. Bleecker**[5], **Mario Castro**[6], **Serpil C. Erzurum**[7], **Benjamin M. Gaston**[8], **Nizar N. Jarjour**[9], **Sally Wenzel**[10], **Eleanor Dunican**[11], **John V. Fahy**[11], **Daniel Irimia**[3], **Denisa D. Wagner**[2], **Bruce D. Levy**[1,*], and **National Heart Lung and Blood Institute Severe Asthma Research Program-3 Investigators**

[1]Pulmonary and Critical Care Medicine Division, Department of Medicine, Brigham and Women's Hospital and Harvard Medical School, Boston, MA 02115, USA.

[2]Program in Cellular and Molecular Medicine, Division of Hematology and Oncology, Boston Children's Hospital, Boston, MA, USA;

[3]BioMEMS Resource Center, Massachusetts General Hospital, Harvard Medical School, MA, USA.

[4]Division of Statistics and Bioinformatics, Department of Public Health Sciences, Pennsylvania State University, Hershey, PA 17033, USA.

[5]Center for Genomics and Personalized Medicine Research, School of Medicine, Wake Forest University Winston-Salem, NC 27157, USA.

[6]Division of Pulmonary and Critical Care Medicine, Departments of Medicine and Pediatrics, Washington University, St. Louis, MO 63110, USA.

[7]Department of Pathobiology, Cleveland Clinic, Cleveland, OH 44195, USA.

[8]Department of Pediatrics, Rainbow Babies and Children's Hospital, Case Western Reserve University, Cleveland, OH 44106, USA.

[9]Section of Pulmonary and Critical Care Medicine, University of Wisconsin School of Medicine, Madison, WI 53792, USA.

[10]Pulmonary, Allergy and Critical Care Medicine Division, Department of Medicine, University of Pittsburgh School of Medicine, Pittsburgh, PA 15213, USA.

[*]Corresponding Author: Dr. Bruce D. Levy, 75 Francis Street, Boston, Massachusetts, 02115, USA. Phone: 617-525-5407; Fax: 617-732-7421; blevy@bwh.harvard.edu.

[¶]These authors contributed equally to the work.

COMPETING INTERESTS:

The authors declare that they have no competing interests.

DATA AND MATERIALS AVAILABILITY:

All data supporting the findings of this study are available within the article.

[11]Division of Pulmonary and Critical Care Medicine, Department of Medicine and the Cardiovascular Research Institute, University of California San Francisco, San Francisco, CA, 94143 USA.

Abstract

Severe asthma is a debilitating and treatment refractory disease. As many as half of these patients have complex neutrophil predominant lung inflammation that is distinct from milder asthma with type 2 eosinophilic inflammation. New insights into severe asthma pathogenesis are needed. Here, concomitant exposure of mice to an aeroallergen and endotoxin during sensitization resulted in complex neutrophilic immune responses to allergen alone during later airway challenge. Unlike allergen alone, sensitization with allergen and endotoxin led to NETosis. Interestingly, in addition to NETs, enucleated neutrophil cytoplasts were evident in the lungs. Surprisingly, allergen-driven airway neutrophilia was decreased in PAD4 deficient mice with defective NETosis, but not by DNAse treatment, implicating the cytoplasts for the non-type 2 immune responses to allergen. Neutrophil cytoplasts were also present in mediastinal lymph nodes and the cytoplasts activated lung dendritic cells *in vitro* to trigger antigen-specific IL-17 production from naïve $CD4^+$ T cells. Bronchoalveolar lavage fluid from patients with severe asthma and high neutrophil counts had detectable NETs and cytoplasts that were positively correlated with IL-17 levels. Together, these translational findings have identified neutrophil cytoplast formation in asthmatic lung inflammation and linked the cytoplasts to Th17 mediated neutrophilic inflammation in severe asthma.

One sentence summary:

Neutrophil cytoplasts promote Th17 inflammation.

INTRODUCTION

Asthma is a common inflammatory disorder of the airways with several underlying endotypes and excess morbidity(1–4). About 10% of patients have severe disease, which responds poorly to corticosteroids and can be associated with neutrophil predominant inflammation and high interleukin (IL)-17 levels(5–8).

In response to inflammatory stimuli, neutrophils form neutrophil extracellular traps (NETs). NETosis releases DNA-containing NETs from cells that may result in the formation of enucleated cell bodies called cytoplasts(9). When nuclei are removed *ex vivo*, neutrophil cytoplasts remain viable and demonstrate some residual cell functions(10–12). Extracellular DNA in NETs has vital roles in host defense (9, 13), yet these structures are also associated with organ injury and inflammation(14, 15). Roles for cytoplasts and NETs in asthma pathogenesis remain to be determined.

Here, in a preclinical model of allergic lung inflammation that incorporates both type 2 and non-type 2 immune responses, we identified neutrophil-derived cytoplasts in lungs and mediastinal lymph nodes. Cytoplasts activated lung dendritic cells to differentiate naïve $CD4^+$ T cells to antigen-specific Th17 effectors. Some bronchoalveolar lavage fluids (BALF) collected from severe asthmatic patients had NETs and cytoplasts that were

associated with increased IL-17 and BAL neutrophils. These findings have identified NETosis-derived cytoplasts *in vivo* and a pivotal mechanism for the cytoplasts to bridge innate and adaptive immune responses with relevance to non-type 2 inflammation in severe asthma pathogenesis.

RESULTS

Neutrophilic inflammation in a murine model of house dust mite extract and endotoxin

Common indoor and outdoor environmental exposures can influence airway inflammation in asthma (16). The presence of endotoxin during allergen sensitization can lead to neutrophilic airway inflammation in mice(17, 18). We established a protocol in which mice were exposed to the common indoor allergen house dust mite (HDM) alone or in combination with lipopolysaccharide (LPS) for 3 days to sensitize the animals, followed by 4 days of rest and then 8 days of intranasal HDM challenge (see Methods, Fig. 1A). While there was no significant difference after HDM challenge in BALF total cell counts between the two different sensitization approaches (Fig. 1B), leukocyte differential cell counts showed significantly higher neutrophil and lower eosinophil numbers in mice sensitized with HDM and LPS (HDM/LPS) compared to HDM and vehicle (HDM/Veh) (Fig. 1C and Supplemental Fig. 1A). Despite 4 days of rest between sensitization with HDM/LPS and airway challenge with HDM alone, BALF neutrophilic inflammation continued to be more prominent than eosinophilia; a response that was distinct from mice sensitized with HDM/Veh. Effector $CD4^+$ T cells were next characterized in the mediastinal lung-draining lymph nodes (MLN). At 4 days post sensitization (Fig. 1a, day 7), there was a significantly higher number of Th17 cells in HDM/LPS sensitized mice compared to HDM/Veh (Fig. 1D, E, and Supplemental Fig. 1B).

Exposure to LPS and allergen promoted NETosis

Instillation of LPS in mouse airways can induce NETosis (14, 19, 20), so BALF were obtained one day after sensitization to address this possibility (day 3, Fig. 2A). Significantly higher numbers of BALF cells were present with HDM/LPS sensitization compared to HDM/Veh (Fig. 2B) with predominant BALF neutrophilia (Fig. 2C and Supplemental Figure 1C). Of note, some of the recruited neutrophils underwent NETosis in the lung as evidenced by increased BALF DNA (Fig. 2D) and hyper-citrullinated histone H3 (Fig. 2E). Cytoplasts are largely devoid of DNA, so the presence of DNA in cells was tracked by flow cytometry using a cell permeable DNA dye. Analyses of BALFs revealed the presence of $CD45^+CD11b^+Ly6G^+DNA^+$ neutrophils and $CD45^+CD11b^+Ly6G^+DNA^-$ cytoplasts from HDM/LPS exposed mice immediately post-sensitization (Fig. 2F and gating strategy in Supplemental Figure 2). Of interest, MLN at protocol day 3 also had $CD45^+CD11b^+Ly6G^+DNA^-$ cytoplasts (Fig. 2G, H and Supplemental Figure 1D). Together, these data indicate that concomitant allergen and LPS exposure but not allergen alone triggered NETosis in the lung with both DNA and cytoplasts present *in vivo*. In addition to lung, cytoplasts were in MLN where allergen exposure skewed effector T cells towards Th17 differentiation.

To determine the role of IL-17 following HDM/LPS exposure, mice were given an anti-IL-17 antibody or control antibody (80μg per mouse, intraperitoneal route) prior to and

during the sensitization phase (protocol day −1 and day 1, Supplemental Figure 3A). After challenge with HDM, the mice sensitized in the presence of the anti-IL-17 antibody had reduced BALF total cell numbers with a significant decrease in BALF neutrophils and concomitant increase in eosinophils (Supplemental Figure 3B). Exposure to the anti-IL-17 antibody did not have a significant effect on lung cytoplast numbers after sensitization (Supplemental Figure 3C). Together, these findings indicate that IL-17 production is downstream of NETosis but pivotal to lung neutrophil accumulation with later allergen challenge.

DNase instillation altered levels of NETs, but not neutrophilia

To address the potential impact of NET DNA, DNase was instilled during sensitization to disrupt the NETs in HDM/LPS exposed mice. DNase led to a significant decrease in NETs compared to PBS control (Fig. 3A and B). With DNase, there was a modest decrease in BALF cells after HDM challenge (day 15; Fig. 3C) without significant changes in the percent or number of BALF neutrophils (Fig. 3D and E). Macrophages and eosinophils were reduced in part, suggesting a potential role for NETs in the recruitment of these cells (Fig. 3D and E). Protease-free DNase (21) gave similar partial decrements in BALF macrophages without significant decreases in BALF neutrophils (Supplemental Figure 4), consistent with a role for the cytoplasts rather than the NETs in neutrophilia after allergen challenge.

Neutrophil cytoplasts retained functional properties

To investigate whether the cellular remnants of NETosis have a functional role in responses to the environmental stimuli (i.e., HDM and LPS), cells were first sorted from murine lungs 3 days following HDM/LPS administration and then cellular responses were evaluated. Neutrophils and enucleated cytoplasts were identified, and the majority of both cell types excluded trypan blue dye (>95%). Neutrophils (average diameter 6.9μm) were significantly larger than the cytoplasts (average diameter: 3.3μm) that had expelled their DNA (Fig. 4A, B). Of note, the cytoplasts were significantly larger than microvesicles (~200 nm), exosomes (~100 nm) and cellular debris. To assess chemotaxis, the sorted cells were placed in a microfluidics device with a gradient established to LTB_4 (100 nM). The cytoplasts displayed chemokinesis, but in contrast to neutrophils did not exhibit chemotaxis to LTB_4 (see Supplemental movies 1 and 2; Fig. 4C–F). The cytoplasts moved more slowly than the neutrophils (Fig. 4G) and displayed random movement despite the LTB_4 chemotactic gradient (Fig. 4H).

The cytoplast chemokinesis suggested an intact cytoskeleton, so phagocytosis was next assessed. After sorting, the cells were incubated with pHrodo-tagged *E. coli* particles that fluoresce after engulfment upon pH change in acidic phagolysosomes (see Methods). Prior to incubation, the absence of nuclei in the cytoplasts was confirmed by DAPI stain (Fig. 4I). After 1 hr, phagocytosis for both the cytoplasts and neutrophils was evident (Fig. 4J). The phagocytosis index was similar for each cell type (Fig. 4K). To assess their capacity for killing a lung relevant pathogen, sorted cytoplasts and neutrophils were incubated with *Streptococcus pneumoniae* (serotype 1). Of note, the cytoplasts displayed killing of the bacteria to a comparable extent as autologous neutrophils (Fig. 4L). Together, these data

indicate that the cytoplasts display several preserved functional responses of their parent neutrophils.

Deficiency in PAD4 resulted in reduced cytoplast generation and IL-17 levels

Because DNAse did not impact neutrophil responses to allergen challenge and cytoplasts retained select cellular functions, we next turned to peptidyl arginine deiminase 4 deficient mice (PAD4 KO) with defective NETosis (22). PAD4 hyper-citrullinates histones and is involved in NETosis (22, 23). After sensitization with HDM/LPS, PAD4 KO mice had reduced numbers of BALF total cells (day 3; Fig. 5A) and neutrophils (Fig. 5B). Western blots of lung homogenates showed decreased hyper-citrullinated histone H3 in PAD4 KO mice during HDM/LPS sensitization (Fig. 5C and D). By flow cytometry criteria (see Methods), cytoplast numbers were also much decreased in the PAD4 KO (Fig 5E and F), suggesting decreased NETosis in PAD4 KO mice in response to HDM/LPS. Also of interest, approximately 7% of WT neutrophils were CitH3^{+} by flow cytometry, indicative of an association with NETs (Supplemental Figure 5). The numbers of citH3^{+} neutrophils in PAD4 KO mice were substantially decreased and neutrophil cytoplasts were citH3^{-} (Supplemental Figure 5). Upon HDM challenge, BALF total cell counts in PAD4 KO were significantly lower than WT mice (Fig. 5G), and BALF neutrophil counts were significantly decreased (Fig. 5H). Changes in BALF eosinophils were not significant (Fig. 5H). After HDM/LPS sensitization and HDM challenge, lung histology was notable for decreased inflammation in PAD4 KO mice relative to WT mice (Fig. 5I). The PAD4 KO mice also had decreased airway mucous cell metaplasia (by PAS stain) (Fig. 5J) and decreased methacholine-induced airway hyper-responsiveness (AHR) compared to WT mice (Fig. 5K). Cytokine production from lung cells following HDM challenge from the two groups of mice was compared. PAD4 KO mice displayed lower levels of cellular IL-17 and IFN-γ (Fig. 5L). Interestingly, type 2 cytokines were not significantly changed in the PAD4 KO mice (Fig. 5M). Together, these data indicate that cytoplasts produced by NETosis during HDM/LPS sensitization were related to an adaptive inflammatory response characterized in part by neutrophilic lung inflammation and IL-17 and IFN-γ production in response to the HDM challenge.

Airway cytoplasts elicited IL-17 production by antigen-specific T lymphocytes

If NETosis-derived cytoplasts could direct neutrophil-enriched adaptive inflammatory responses, then cytoplasts and neutrophils should have distinct effects on allergen-initiated inflammation. To test this hypothesis, lung dendritic cells (DCs) were isolated from HDM/LPS and HDM/Veh sensitized mice for incubation with cytoplasts or neutrophils prior to naïve T cells from DO11.10 mice in the presence of ovalbumin peptide (Fig. 6A). In this *in vitro* reporter assay of cell-cell interactions for antigen presentation and DC initiation of adaptive T cell effector responses, there was a higher abundance of antigen-specific CD4^{+} Th17 T cells with cytoplasts compared to neutrophils (Fig. 6B). The cytoplast-mediated skewing to Th17 was dose dependent for the two DC:cytoplast cell ratios tested (1:0.5 and 1:2) and greater than that observed with DC:neutrophil ratio of 1:0.5, 1:2 and even an excess ratio of 1:10 (Fig. 6B, Supplemental Figure 6). DCs from both HDM/LPS and HDM/Veh had similar responses, supporting a pivotal role for the cytoplasts in Th17 differentiation. Because cytoplasts were present in BALF and MLN (Fig. 1), these results suggest that

cytoplasts, but not neutrophils, in proximity to DCs can directly educate DCs to induce antigen-specific Th17 differentiation. Of interest, the cytoplasts also triggered the expression of IL-13 from $CD4^+$ T cells, although to a lesser extent than IL-17 (Fig. 6B). The DC:cytoplasts interaction was contact-dependent to trigger IL-17 and IL-13 production, as the antigen-specific cytokine generation *in vitro* was abrogated when the cytoplasts were separated from DCs and T cells with a transwell culture system (Supplemental Figure 6). Conditioned media from cytoplast culture (24 hours) also failed to promote IL-17 and IL-13 production by the T cells (Supplemental Figure 6). The data from these experiments highlight a bridging function for cytoplasts in programing an adaptive immune response in T cells that is contact-dependent and distinct from neutrophils.

Select cytoplast surface proteins are distinct from intact neutrophils.

To begin to dissect the distinct DC responses to cytoplasts and neutrophils, several surface proteins on cytoplasts and neutrophils were analyzed by flow cytometry. Both cytoplasts and neutrophils displayed very low levels of annexin V expression (Fig. 7), and expression of CD32(FcyRII) was below the limits of detection on both cell populations. The expression of TLR4 on neutrophils and cytoplasts was comparable (Fig. 7). Of note, cytoplasts did not significantly express DC-SIGN(CD209), but cytoplasts did display substantial expression of MHCII, which was in contrast with neutrophils (Fig. 7). Even with this limited array of surface proteins, it is evident that there are select differences in cytoplasts and neutrophils that may account for their distinct and overlapping functions.

Cytoplasts correlated with IL-17 levels in the BAL fluid of severe asthmatics

To determine if NETosis was operative in human asthma, we first measured DNA levels in bronchoalveolar lavage fluids (BALF) from subjects with severe asthma (SA) (n=41), non-severe asthma (NSA) (n=28) and healthy donors (HD) (n=25) in the National Heart, Lung and Blood Institute's severe asthma research program–3 (SARP-3)(Supplemental Table 1). BALF DNA was measurable in a subset of asthmatic individuals (Fig. 8A), in particular in samples from patients meeting SARP-3 criteria for severe asthma (see Methods). Increased levels of DNA in severe asthma were principally identified in BALFs with neutrophils ≥5% (Fig. 8B). To more confidently identify DNA from NETosis, hyper-citrullinated histone H3 was detected by Western blot in severe asthma BALF with high neutrophil counts (Fig. 8C). BALF levels of DNA in severe asthma were strongly correlated with neutrophil count (Fig. 8D). In addition to BALF DNA, BAL cells from severe asthma (n=28) and non-severe asthma (n=19) subjects were analyzed for cytoplasts by flow cytometry. Cytoplasts were identified as $CD45^+CD66b^+CD16^+DNA^-$ with low side scatter (gating strategy in Supplemental Figure 7). There was a strong positive correlation between BAL neutrophils and cytoplasts and both cell types were associated with BALF IL-17 levels (Fig. 8E and 8F). Of the asthmatic patients with high BAL neutrophils and DNA, there was an increased association with frequent asthma exacerbations (>4 per year) and sinusitis (Supplemental Table 2). Together, these translational findings indicate that a subset of severe asthmatic individuals with neutrophil-predominant inflammation have active lung NETosis with an association between cytoplasts and IL-17 levels, suggesting that similar to the preclinical model with HDM/LPS (Fig. 1–3) these enucleated cytoplasts can skew an adaptive immune response towards Th17 to propagate lung neutrophilia.

DISCUSSION

Asthma is a heterogeneous disorder (2, 24, 25). While eosinophilia and type 2 inflammation are prominent in at least 50% of asthma, some severe asthmatic patients have substantial neutrophilia that is likely to indicate distinct pathogenic mechanisms (26–28). To understand how LPS exposure during sensitization could influence later responses to allergen challenge, we characterized the acute responses to sensitization and identified a marked increase in lung neutrophils and NETosis in the animals exposed to allergen with LPS. Of interest, in addition to NETs, the resulting neutrophil cytoplasts were also detectable in lung and mediastinal lymph nodes. PAD4 KO mice had reduced NETosis during sensitization and decreased neutrophils and Th17 responses to later allergen challenge. DNAse treatment decreased BALF DNA levels and lung macrophages; however, lung neutrophils were not decreased. There was a trend for reduced allergen-initiated BAL eosinophilia that did not reach significance. Together, these findings implicate the neutrophil cytoplasts as an underlying mechanism for the allergen-mediated Th17 responses. Interestingly, administration of neutralizing antibody for either IL-17A or IL-17F given during allergen sensitization can attenuate murine allergic lung inflammation and airway hyperreactivity (29) and here administration of anti-IL-17 antibody during the sensitization phase significantly decreased BAL total leukocytes and neutrophilia. IL-17 neutralizing antibody did not impact lung cytoplast numbers, supporting a role for IL-17A downstream from cytoplasts for allergen-initiated lung neutrophil recruitment. With neutrophils and neutrophil cytoplasts present in respiratory tissues, immune functions for both cell types were examined after isolation by FACS. The enucleated cytoplasts were smaller in size compared to neutrophils, and retained membrane integrity (i.e., excluded trypan blue). Albeit smaller than neutrophils, the cytoplasts (3–4.5 μm) were significantly larger than microvesicles or exosomes. The isolated cytoplasts were chemokinetic but differed from neutrophils by not exhibiting chemotaxis to LTB_4. The cytoplasts were mobile in the microfluidic chamber and exhibited random motion via pseudopods, consistent with the published properties of neutrophil cytoplasts from NETosis during bacterial infection (9). The phagocytic index of the cytoplasts for *E.coli* particles and for killing *Streptococcus pneumoniae* was comparable to neutrophils and similar to properties of neutrophil cytoplasts generated by *ex vivo* enucleation, which remain capable of phagocytosis of staphylococci(30–32). The phagocytic capacity of neutrophil cytoplasts after NETosis suggests sufficiently intact cytoskeleton and membrane integrity for functional cell responses. The comparable TLR4 staining in cytoplasts and neutrophils following LPS exposure also suggests a similar mechanism for sensing gram negative bacteria. Of note, NETosis and neutrophil cytoplasts have also been detected with Gram-positive bacteria, suggesting the presence of other TLR molecules on cytoplasts.

Dendritic cells are critical antigen presenting cells that instruct $CD4^+$ T cells to differentiate with a specific phenotype (33). The cytoplasts chemokinesis and their presence in the mediastinal lymph nodes suggested cytoplast trafficking via lung lymphatics and their potential for spatiotemporal regulation of T cell priming. When cytoplasts were incubated with dendritic cells, they promoted differentiation of naive $CD4^+$ T cells to produce IL-17 in an antigen-specific and dose-dependent manner. The levels of IL-17 induced by the

cytoplasts were approximately 2-fold higher than IL-13. Of note, neutrophils did not trigger this Th17 immune response, suggesting that dendritic cells were responding to the activated cytoplasts in a distinct manner than to the intact neutrophils. The antigen-specific nature of this response supports a directed role for this cell-cell interaction between the dendritic cells and cytoplasts that is not simply a generalized alarm signal. Interestingly, increased expression of MHCII on cytoplasts indicates the potential capacity to process and present antigen. The loss of augmented IL-17 and IL-13 production when DCs and cytoplasts were separated in culture by transwell suggests that antigen presentation via MHCII during cytoplast contact with DCs is a potential mechanism for cytoplast-mediated DC programing of T cell cytokine production. One caveat is that adherent NET fragments on cytoplasts cannot be entirely excluded. If present, cytoplast-associated surface DNA would be another potential mechanism for cell activation. DC-SIGN expression on cytoplasts was low, so the mechanisms for T cell skewing to IL-17 production were likely independent of DC-SIGN. The ability of neutrophil cytoplasts to trigger a regulated Th17-driven immune response is reminiscent of prior reports that infected apoptotic cells can also promote Th17 differentiation (34).

To translate the murine findings to human asthma, BAL samples from comprehensively phenotyped healthy and asthmatic subjects were studied. DNA, including hyper-citrullinated histones consistent with NETs, was present in a subset of severe asthmatic patients with high BAL neutrophil counts. In severe asthma, BALF levels of DNA correlated to BAL neutrophils. Neutrophil cytoplasts were also detected in severe asthma BAL with high neutrophil counts. BAL neutrophils and cytoplasts correlated with BALF levels of IL-17. Compared to asthmatics with lower BAL neutrophil counts, the asthma patients with increased BAL neutrophils and NETosis were associated with frequent exacerbations and sinusitis – asthma co-morbidities linked to infections. Together, these findings support the notion that a subset of severe asthmatic patients has neutrophil-enriched inflammatory responses that are driven by cytoplast skewing to Th17 adaptive inflammation. Several studies have identified NETs in biospecimens from asthmatic subjects (35) and some have linked the DNA to type 2 responses (36). In sharp contrast, intact neutrophil cytoplasts after NETosis have not been previously detected in human asthma or after murine responses to allergen. Neutrophil cytoplasts have been detected after NETosis *in vivo* with murine gram positive bacterial infection and in human gram positive abscesses (9), suggesting that the findings here have uncovered a mechanistic link between innate and adaptive immune responses that is relevant more broadly to neutrophilic diseases. Many severe asthmatic patients do not benefit from anti-inflammatory therapy with corticosteroids, which can prolong neutrophil survival and delay their clearance from asthmatic lungs (37, 38). A phase 2a anti-IL-17 receptor A antibody clinical trial did not demonstrate improvement in asthma symptoms in moderate to severe asthmatics (39); however, stratification of the asthmatic subjects by neutrophils and IL-17 levels was not performed. Markers of NETosis, such as DNA-citrullinated histones or neutrophil cytoplasts in sputum, may provide an opportunity for increased precision or alternate therapeutic strategies to disrupt IL-17 pathways in subsets of asthma patients in future clinical research.

In summary, during allergen mediated responses, the presence of endotoxin can trigger lung NETosis with functional roles for the enucleated cytoplasts to convey specific signals of

neutrophil activation that can serve as pivotal effectors for initiation of Th17 differentiation in a transition from innate to adaptive immune responses. Cell-cell interactions between neutrophil cytoplasts and dendritic cells are spatiotemporally regulated and can elicit antigen-specific T cell responses with direct relevance to disease pathogenesis for some patients with severe asthma and non-type 2 inflammation. Our translational results also suggest a broader role for NETosis-derived cytoplasts in initiating Th17-driven adaptive immune responses to pathogens that are crucial to host defense.

Online Methods

Mice

Balb/c mice used for the asthma model were purchased from Charles River. C57BL/6 mice, C.Cg-Tg(DO11.10)10Dlo/J mice and control BALB/c mice were purchased from The Jackson Laboratory. PAD4 KO mice (22) (C57BL/6 background) were obtained as a gift from Dr. Yanming Wang's laboratory and were bred at Boston Children's Hospital. The mice were backcrossed for more than 10 generation on the C57BL/6 background. Unless otherwise stated, age matched male animals were used at 8 – 12 weeks of age. The animal protocols were approved by the Animal Review Committee at Harvard Medical School and Boston Children's Hospital.

15-day model of allergic lung inflammation

For the intranasal instillations, animals were sedated using isoflurane carried by oxygen. For allergen sensitization, 25 μg of HDM (B70 source material, Greer labs) with or without 1 μg LPS (*E. coli* O55:B5, Sigma) was instilled (i.n.) in 30 μl normal saline once daily for three days (days 0 – 2). In some experiments, mice were sacrificed on day 3 and bronchoalveolar lavage (BAL) was performed using PBS containing 0.6 mM EDTA. MLN were also harvested on day 3 from some mice for analyses.

In other experiments, DNase (500 μg/mouse in 50 μl PBS) or PBS control was instilled intranasally 6 h post each sensitization (days 0 – 2). For allergen challenge, mice were rested for 4 days after sensitization (days 3 – 6). In some experiments, MLN were harvested on day 7 to study T lymphocyte differentiation. Beginning on day 7, 25 μg of HDM in 25 μl saline was instilled (i.n.) once daily for 8 days (days 7 – 14). Mice were then sacrificed 24 hours later on day 15, BAL was performed and MLN were harvested for analyses. BAL fluids (BALFs) were centrifuged (400 μ g, 10 min). Cell pellets were re-suspended for analysis by flow cytometry or cytospin and staining with Diff Quik stain to determine leukocyte differential counts.

In the anti-IL-17 experiments, two doses of anti-IL-17A (ThermoFisher; clone eBioMM17F3) or control rIgG were administered to the mice (80μg, 100μL) via the intraperitoneal route 24 hours prior to the first sensitization with HDM/LPS (protocol day −1) and then during HDM/LPS sensitization (protocol day 1, Supplemental Figure 3A). The sensitization phase was completed with HDM/LPS followed by challenge with HDM. 24h after the last HDM challenge, the cellular profile in the BAL fluid was analyzed.

For airway hyperresponsiveness, the protocol was performed as described previously (40). Briefly, anesthetized mice were mechanically ventilated using a flexiVent (SciReq) and aerosolized methacholine (0, 3, 10, and 30 mg/ml) was delivered in-line via the inhalation port for 10 sec. Lung resistance was calculated to the baseline dose of methacholine (dose 0, PBS control).

Cell-free supernatants were subjected to analysis by Quant-It PicoGreen double strand DNA quantitation assay (Thermo Fisher) or immunoblot analysis for hyper-citrullinated histone H3 to detect NETs. For western blot, rabbit polyclonal Ab to histone H3 (citrulline 2 + 8 + 17, Abcam) was used. For MLN T lymphocyte analysis, MLN were dissociated to achieve single cell suspensions using 5 ml polypropylene round bottom tube with 0.3 μm filter cap. Harvested MLN were crushed using the plunger of 1 ml syringe and ice-cold PBS with 2 % heat inactivated FBS. Cells from day 3 mice were then counted and analyzed for neutrophil and cytoplast infiltration. MLN cells harvested from day 7 mice were counted, and 2 μ 10^6 cells in 2 ml of RPMI with 10 % FBS, 1 mM Na pyruvate, 1 μ penicillin/streptomycin mix and 5 μg/ml gentamicin. MLN cells were then re-stimulated with PMA (50 ng/ml), ionomycin (500 ng/ml) and GolgiStop for 96 h at 37°C in a humidified incubator with 5 % CO_2. Cells were then harvested, dissociated and stained for intracellular cytokine staining using FoxP3 Staining Kit (eBioscience) as per the manufacturer's protocol.

Flow cytometry

Cell suspensions were stained in ice cold PBS with or without 2 % FBS on ice. The following antibodies were used for staining mouse cells: CD45 (clone 30-F11, Biolegend), Ly6G (clone 1A8, BD Biosciences), CD11c (clone HL3, BD Biosciences), CD11b (clone M1/70, Biolegend), Siglec F (clone E50–2440, BD Biosciences), CD3e (clone 145–2C11, eBioscience), CD4 (clone GK1.5, Biolegend), IFN © (clone XMG1.2, Biolegend), IL-17 (clone eBio17B7, eBioscience), IL-5 (clone TRFK5, Biolegend), IL-13 (clone eBio13A, eBioscience), CD25 (clone PC61.5, eBioscience), CD44, CD62L (clone MEL-14, BD Biosciences), MHC class II I-A/I-E (clone M5/114.15.2, eBioscience), DC-SIGN/CD209 (R&D systems), CD32 (clone D34–485, eBioscience), TLR4/CD284 (clone SA15–21, Biolegend), Annexin V (Biolegend). Neutrophils were defined as $CD45^+CD11b^+Ly6G^+DNA^+$ and cytoplasts were defined at $CD45^+CD11b^+Ly6G^+DNA^-$. Naïve T lymphocytes were defined as $CD4^+CD25^-CD44^{low}CD62L^{hi}$. Lung Dendritic cells were defined as $CD45^+CD11c^+$ $MHCII^+autofluorescence^{low}$. The following antibodies were used to stain human cells: anti-CD45 PE-Cy7 (HI30), anti-CD66b (G10F5), anti-CD16 APC-Cy7 (3G8) all from Biolegend. Vybrant DyeCycle Ruby (Life Technologies) was used to stain intracellular DNA. Data were acquired on BD Canto II or BD LSR Fortessa and analyzed using FlowJo v10. For cell sorting, FACS Aria was used.

Neutrophil/cytoplast, DC, and T cell co-culture assay

Two cohorts of mice were sensitized with HDM/LPS and HDM/Veh. Mice were sacrificed on day 3. BAL was performed in one cohort, and $CD45^+CD11b^+Ly6G^+DNA^+$ neutrophils and $CD45^+CD11b^+Ly6G^+DNA^-$ cytoplasts were flow sorted from BALFs. From second cohort, harvested lugs were dissociated and $CD45^+CD11c^+MHCII^+$ dendritic cells (DCs) were flow sorted. These DCs were then co-cultured with either cytoplasts (DC:cytoplast cell

ratios of 1:0.5 or 1:2) or neutrophils (DC:neutrophil cell ratio of 1:0.5, 1:2 or 1:10) overnight. The next day, the spleens of DO11.10 were harvested, and crushed using 70μm cell strainer and plunger from a 5 ml syringe with ice cold PBS with 2 % FBS to obtain single cell suspension. Cells were then centrifuged (800 μ g, 6 min, 4°C). Red blood cells were then lysed using RBC lysis buffer (eBioscience) as per the manufacturer's instructions. Cells were then washed and re-suspended in PBS with 2 % FBS, stained and sorted for $CD4^+CD25^-CD44^{lo}CD62L^{hi}$ naïve T lymphocytes. Naïve T lymphocytes were then added to the DCs (10:1, T cells:DC), together with ovalbumin peptide (5 μg/ml). In select experiments the cytoplasts were separated from the DC:T cells by transwell. The cytoplasts were added to the transwell allowing the flow of the media but preventing the cytoplasts from directly interacting with DCs and T cells. Additionally, conditioned supernatant from cytoplast culture for 24 hours was added to the DC: T cell co-culture to determine the potential role of soluble factors from cytoplasts in T cell differentiation. The cells were then cultured for 96 h and T cell differentiation was assessed by re-stimulating with PMA (50 ng/ml), ionomycin (500 ng/ml) and GolgiStop. Cells were then harvested, dissociated and stained for intracellular cytokine staining using FoxP3 Staining Kit (eBiosciences) as per the manufacturer's protocol.

Design and fabrication of the microfluidic assay.—The *in vitro* microfluidic assay enables investigation of chemotaxis of neutrophils and cytoplasts with high temporal and spatial resolution. It has three key components, (1) cell loading channel, (2) chemoattractant chambers, and (3) an array of migration channels which bridge the first two components. The cell loading channel and the chemoattractant chambers have a dimension of 200 μm × 100 μm ($h \times w$). The migration channels have a dimension of 10 μm × 10 μm × 500 μm ($h \times w \times l$). Each device has 10 identical units with a total number of 90 migration channels, which allows observation of hundreds of cells in one experiment.

Device priming.: First, the microfluidic device was placed in a desiccator under vacuum for 20mins to generate a negative pressure in the device. Immediately after the degassing process, 5 μL of cRPMI media containing 100nM LTB_4 (Cayman Chemical, Ann Arbor, MI) and 100nM fibronectin (R&D Systems Inc., Minneapolis, MN) was introduced into the cell loading channel through the inlet port using a pipette. The temporary negative pressure pulled the media into the migration channels and chemoattractant chambers filling the device within 10 min. The cell loading channel was then washed with 10 μL fresh media to establish a chemogradient from the chemoattractant chambers (highest chemokine concentration) to the cell loading channel (lowest chemokine concentration). 1μL mice neutrophils or cytoplasts at a concentration of 2×10^7/mL were introduced into a device. Afterward, the device was immersed by pipetting 4mL media into the well and was ready for the following time-lapse imaging.

Time-lapse imaging and analysis.: The 6-well plate was mounted on a Nikon Eclipse Ti microscope equipped with a biochamber to maintain the temperature and gas conditions at 37°C and 5% CO_2. For each condition, 20 images were taken at different locations in 2 identical devices using a 10× lens in bright field. The experiment was imaged for 6 hr with a 3 min interval between 2 imaging cycles. The sizes of neutrophils and cytoplasts were

measured using FIJI imageJ. The recruitment of neutrophils or cytoplasts was analyzed by counting the number of cells that entered the migration channels. The velocities and trajectories of neutrophil chemotaxis and cytoplast chemokinesis were measured using Trackmate in FIJI imageJ.

Phagocytosis assay

Neutrophils and cytoplasts were cell sorted (see cell sorter methods) and plated on serum-coated slides (10^5 cells per slide). The cells were allowed to adhere on the slides at 37°C for 1 hr. *E. coli* particles conjugated to pHrodo red dye (100 μg/ml, Life Technologies, NY) were added to neutrophils and cytoplasts. Slides were captured with Zeiss epi-fluorescence microscopy with filter sets for indicator dye of pHrodo Red (green excitation) or DAPI (blue excitation) 60 minutes after the addition of *E. coli* particles. Total cell count was obtained by enumerating cells on light microscopy. Phagocytosis index was determined by counting the number of cells stained positive for pHrodo Red relative to total cells.

Bacterial Killing

Frozen stocks of *Streptococcus pneumoniae* were plated and grown for 12 hours at 37ºC, 5% CO_2. Fresh colonies were grown in 10 ml of Todd Hewitt Broth (0.5% of yeast extract) until log phase (O.D. $_{600}$= 0.4 a.u. ~ 1.5×10^9 CFU). After centrifugation (2000 rpm, 20 min), cells were washed with sterile PBS and resuspended in 1 ml of RPMI 5% fetal bovine serum. Sorted neutrophils or cytoplasts were incubated with a 1 ml solution of log-phase *Streptococcus pneumoniae* serotype 1 with an MOI of 2 for 30, 60 and 120 minutes at 37ºC, 5% CO_2. At each time point, 50 μl of the culture supernatant was serial diluted and plated on Blood Agar plates. The plates were incubated overnight at 37ºC, 5% CO_2 and after counting the colonies, results were expressed as CFUs of *S. pneumoniae* per ml.

Human Subjects

Adult patients 18 years of age and older with asthma and healthy controls were recruited to the Severe Asthma Research program-3 (SARP-3, NCT01606826) between November 2012 and October 2014 by seven research centers in the United States. Subjects were defined as having severe or non-severe asthma as defined by the European Respiratory Society/ American Thoracic Society guidelines(41). Healthy subjects were non-smokers with no history of lung disease, atopic disease or allergic rhinitis. Written informed consent was obtained after IRB approval at each site. Bronchoalveolar lavage (BAL) was performed by instilling warm saline (three 50mL aliquots) into the right middle lobe. BALF was recovered and BAL cells and cell-free BAL supernatant were frozen and stored at −80°C or liquid nitrogen and later shipped to Brigham and Women's Hospital for analysis. Subject demographic information is provided in Supplemental Table 1.

BALF IL-17 measurement

IL-17 was measured in cell-free BALF from asthma subjects using a flow cytometry bead-based immunoassay (LEGENDPlex; Biolegend).

Statistics

Results are expressed as mean ± SEM or mean ± SD as stated in the figure legends. Statistical differences were calculated by two-tailed unpaired Student's *t* test between two groups and by parametric one-way ANOVA between three or more groups (human cohorts). For non-normal data distribution, a Mann–Whitney U test or non-parametric one-way ANOVA was used. Correlations were evaluated by Pearson's correlation coefficient (r). For Supplemental Table 2, comparisons between categorical variables were assessed by chi square test. $p < 0.05$ was defined as statistically significant.

Supplementary Material

Refer to Web version on PubMed Central for supplementary material.

ACKNOWLEDGEMENTS:

The authors thank Dr. Guangli Zhu for technical support. We thank Dr. Yiling Qui and Yi-Dong Lin for their technical help with flow cytometry sorting of cells.

FUNDING:

The work was supported in part by the National Heart, Lung, and Blood Institute as follows: Elliot Israel and Bruce Levy, U10 HL109172; Eugene R. Bleecker, U10 HL109164; Mario Castro, U10 HL109257; Serpil Erzurum, U10 HL109250; John Fahy, U10 HL109146; Benjamin Gaston, U10 HL109250; Nizar Jarjour, U10 HL109168; Sally Wenzel, U10 HL109152; David Mauger, U10 HL109086; and by R35HL135765(DWW) and RO1HL122531 (BDL). In addition, this program is supported through the following NIH National Center for Advancing Translational Sciences (NCATS) awards: UL1 TR001420 to Wake Forest University, UL1 TR000427 to the University of Wisconsin, UL1 TR001102 to Harvard University, and UL1 TR000454 to Emory University as well as a CIHR postdoctoral fellowship (DND), K12 HD047349 (MGD), K08 HL130540 (REA); and a fellowship from the German Society for Pediatric Pneumology (IR).

REFERENCES

1. Fanta CH, Asthma. N Engl J Med 360, 1002–1014 (2009). [PubMed: 19264689]
2. Holgate ST, Innate and adaptive immune responses in asthma. Nat Med 18, 673–683 (2012). [PubMed: 22561831]
3. Levy BD, Noel PJ, Freemer MM, Cloutier MM, Georas SN, Jarjour NN, Ober C, Woodruff PG, Barnes KC, Bender BG, Camargo CA, Jr., Chupp GL, Denlinger LC, Fahy JV, Fitzpatrick AM, Fuhlbrigge A, Gaston BM, Hartert TV, Kolls JK, Lynch SV, Moore WC, Morgan WJ, Nadeau KC, Ownby DR, Solway J, Szefler SJ, Wenzel SE, Wright RJ, Smith RA, Erzurum SC, Future Research Directions in Asthma. An NHLBI Working Group Report. Am J Respir Crit Care Med 192, 1366–1372 (2015). [PubMed: 26305520]
4. Wenzel SE, Asthma phenotypes: the evolution from clinical to molecular approaches. Nat Med 18, 716–725 (2012). [PubMed: 22561835]
5. Alcorn JF, Crowe CR, Kolls JK, TH17 cells in asthma and COPD. Annu Rev Physiol 72, 495–516 (2010). [PubMed: 20148686]
6. Al-Ramli W, Prefontaine D, Chouiali F, Martin JG, Olivenstein R, Lemiere C, Hamid Q, T(H)17-associated cytokines (IL-17A and IL-17F) in severe asthma. J Allergy Clin Immunol 123, 1185–1187 (2009). [PubMed: 19361847]
7. Newcomb DC, Cephus JY, Boswell MG, Fahrenholz JM, Langley EW, Feldman AS, Zhou W, Dulek DE, Goleniewska K, Woodward KB, Sevin CM, Hamilton RG, Kolls JK, Peebles RS, Jr., Estrogen and progesterone decrease let-7f microRNA expression and increase IL-23/IL-23 receptor signaling and IL-17A production in patients with severe asthma. J Allergy Clin Immunol 136, 1025–1034 e1011 (2015). [PubMed: 26242299]

8. Wang YH, Wills-Karp M, The potential role of interleukin-17 in severe asthma. Curr Allergy Asthma Rep 11, 388–394 (2011). [PubMed: 21773747]
9. Yipp BG, Petri B, Salina D, Jenne CN, Scott BN, Zbytnuik LD, Pittman K, Asaduzzaman M, Wu K, Meijndert HC, Malawista SE, de Boisfleury Chevance A, Zhang K, Conly J, Kubes P, Infection-induced NETosis is a dynamic process involving neutrophil multitasking in vivo. Nat Med 18, 1386–1393 (2012). [PubMed: 22922410]
10. Malawista SE, Van Blaricom G, Phagocytic capacity of cytokineplasts from human blood polymorphonuclear leukocytes. Blood Cells 12, 167–177 (1986). [PubMed: 3539234]
11. Rich AM, Giedd KN, Cristello P, Weissmann G, Granules are necessary for death of neutrophils after phagocytosis of crystalline monosodium urate. Inflammation 9, 221–232 (1985). [PubMed: 4044026]
12. Roos D, Voetman AA, Meerhof LJ, Functional activity of enucleated human polymorphonuclear leukocytes. J Cell Biol 97, 368–377 (1983). [PubMed: 6309859]
13. Brinkmann V, Zychlinsky A, Neutrophil extracellular traps: is immunity the second function of chromatin? J Cell Biol 198, 773–783 (2012). [PubMed: 22945932]
14. Caudrillier A, Kessenbrock K, Gilliss BM, Nguyen JX, Marques MB, Monestier M, Toy P, Werb Z, Looney MR, Platelets induce neutrophil extracellular traps in transfusion-related acute lung injury. J Clin Invest 122, 2661–2671 (2012). [PubMed: 22684106]
15. Thomas GM, Carbo C, Curtis BR, Martinod K, Mazo IB, Schatzberg D, Cifuni SM, Fuchs TA, von Andrian UH, Hartwig JH, Aster RH, Wagner DD, Extracellular DNA traps are associated with the pathogenesis of TRALI in humans and mice. Blood 119, 6335–6343 (2012). [PubMed: 22596262]
16. Stein MM, Hrusch CL, Gozdz J, Igartua C, Pivniouk V, Murray SE, Ledford JG, Marques dos Santos M, Anderson RL, Metwali N, Neilson JW, Maier RM, Gilbert JA, Holbreich M, Thorne PS, Martinez FD, von Mutius E, Vercelli D, Ober C, Sperling AI, Innate Immunity and Asthma Risk in Amish and Hutterite Farm Children. N Engl J Med 375, 411–421 (2016). [PubMed: 27518660]
17. Arora M, Poe SL, Oriss TB, Krishnamoorthy N, Yarlagadda M, Wenzel SE, Billiar TR, Ray A, Ray P, TLR4/MyD88-induced CD11b+Gr-1 int F4/80+ non-migratory myeloid cells suppress Th2 effector function in the lung. Mucosal Immunol 3, 578–593 (2010). [PubMed: 20664577]
18. Hammad H, Chieppa M, Perros F, Willart MA, Germain RN, Lambrecht BN, House dust mite allergen induces asthma via Toll-like receptor 4 triggering of airway structural cells. Nat Med 15, 410–416 (2009). [PubMed: 19330007]
19. Clark SR, Ma AC, Tavener SA, McDonald B, Goodarzi Z, Kelly MM, Patel KD, Chakrabarti S, McAvoy E, Sinclair GD, Keys EM, Allen-Vercoe E, Devinney R, Doig CJ, Green FH, Kubes P, Platelet TLR4 activates neutrophil extracellular traps to ensnare bacteria in septic blood. Nat Med 13, 463–469 (2007). [PubMed: 17384648]
20. Douda DN, Jackson R, Grasemann H, Palaniyar N, Innate immune collectin surfactant protein D simultaneously binds both neutrophil extracellular traps and carbohydrate ligands and promotes bacterial trapping. J Immunol 187, 1856–1865 (2011). [PubMed: 21724991]
21. Noges LE, White J, Cambier JC, Kappler JW, Marrack P, Contamination of DNase Preparations Confounds Analysis of the Role of DNA in Alum-Adjuvanted Vaccines. J Immunol 197, 1221–1230 (2016). [PubMed: 27357147]
22. Li P, Li M, Lindberg MR, Kennett MJ, Xiong N, Wang Y, PAD4 is essential for antibacterial innate immunity mediated by neutrophil extracellular traps. The Journal of experimental medicine 207, 1853–1862 (2010). [PubMed: 20733033]
23. Wang Y, Li M, Stadler S, Correll S, Li P, Wang D, Hayama R, Leonelli L, Han H, Grigoryev SA, Allis CD, Coonrod SA, Histone hypercitrullination mediates chromatin decondensation and neutrophil extracellular trap formation. J Cell Biol 184, 205–213 (2009). [PubMed: 19153223]
24. Ray A, Raundhal M, Oriss TB, Ray P, Wenzel SE, Current concepts of severe asthma. J Clin Invest 126, 2394–2403 (2016). [PubMed: 27367183]
25. Simpson JL, Grissell TV, Douwes J, Scott RJ, Boyle MJ, Gibson PG, Innate immune activation in neutrophilic asthma and bronchiectasis. Thorax 62, 211–218 (2007). [PubMed: 16844729]
26. Fahy JV, Type 2 inflammation in asthma--present in most, absent in many. Nat Rev Immunol 15, 57–65 (2015). [PubMed: 25534623]

27. Gao P, Gibson PG, Baines KJ, Yang IA, Upham JW, Reynolds PN, Hodge S, James AL, Jenkins C, Peters MJ, Zhang J, Simpson JL, Anti-inflammatory deficiencies in neutrophilic asthma: reduced galectin-3 and IL-1RA/IL-1beta. Respir Res 16, 5 (2015). [PubMed: 25616863]
28. Parfrey H, Farahi N, Porter L, Chilvers ER, Live and let die: is neutrophil apoptosis defective in severe asthma? Thorax 65, 665–667 (2010). [PubMed: 20685738]
29. Chenuet P, Fauconnier L, Madouri F, Marchiol T, Rouxel N, Ledru A, Mauny P, Lory R, Uttenhove C, van Snick J, Iwakura Y, di Padova F, Quesniaux V, Togbe D, Ryffel B, Neutralization of either IL-17A or IL-17F is sufficient to inhibit house dust mite induced allergic asthma in mice. Clinical science (London, England : 1979) 131, 2533–2548 (2017).
30. Malawista SE, Montgomery RR, van Blaricom G, Evidence for reactive nitrogen intermediates in killing of staphylococci by human neutrophil cytoplasts. A new microbicidal pathway for polymorphonuclear leukocytes. J Clin Invest 90, 631–636 (1992). [PubMed: 1379614]
31. Malawista SE, Montgomery RR, Van Blaricom G, Microbial killing by human neutrophil cytokineplasts: similar suppressive effects of reversible and irreversible inhibitors of nitric oxide synthase. Journal of leukocyte biology 60, 753–757 (1996). [PubMed: 8975878]
32. Malawista SE, Van Blaricom G, Breitenstein MG, Cryopreservable neutrophil surrogates. Stored cytoplasts from human polymorphonuclear leukocytes retain chemotactic, phagocytic, and microbicidal function. J Clin Invest 83, 728–732 (1989). [PubMed: 2536406]
33. Merad M, Sathe P, Helft J, Miller J, Mortha A, The dendritic cell lineage: ontogeny and function of dendritic cells and their subsets in the steady state and the inflamed setting. Annual review of immunology 31, 563–604 (2013).
34. Torchinsky MB, Garaude J, Martin AP, Blander JM, Innate immune recognition of infected apoptotic cells directs T(H)17 cell differentiation. Nature 458, 78–82 (2009). [PubMed: 19262671]
35. Wright TK, Gibson PG, Simpson JL, McDonald VM, Wood LG, Baines KJ, Neutrophil extracellular traps are associated with inflammation in chronic airway disease. Respirology (Carlton, Vic.) 21, 467–475 (2016).
36. Toussaint M, Jackson DJ, Swieboda D, Guedan A, Tsourouktsoglou TD, Ching YM, Radermecker C, Makrinioti H, Aniscenko J, Edwards MR, Solari R, Farnir F, Papayannopoulos V, Bureau F, Marichal T, Johnston SL, Host DNA released by NETosis promotes rhinovirus-induced type-2 allergic asthma exacerbation. Nat Med, (2017).
37. Duvall MG, Barnig C, Cernadas M, Ricklefs I, Krishnamoorthy N, Grossman NL, Bhakta NR, Fahy JV, Bleecker ER, Castro M, Erzurum SC, Gaston BM, Jarjour NN, Mauger DT, Wenzel SE, Comhair SA, Coverstone AM, Fajt ML, Hastie AT, Johansson MW, Peters MC, Phillips BR, Israel E, Levy BD, Natural killer cell–mediated inflammation resolution is disabled in severe asthma. Science Immunology 2, (2017).
38. Wang M, Gao P, Wu X, Chen Y, Feng Y, Yang Q, Xu Y, Zhao J, Xie J, Impaired anti-inflammatory action of glucocorticoid in neutrophil from patients with steroid-resistant asthma. Respir Res 17, 153 (2016). [PubMed: 27852250]
39. Busse WW, Holgate S, Kerwin E, Chon Y, Feng J, Lin J, Lin SL, Randomized, double-blind, placebo-controlled study of brodalumab, a human anti-IL-17 receptor monoclonal antibody, in moderate to severe asthma. Am J Respir Crit Care Med 188, 1294–1302 (2013). [PubMed: 24200404]
40. Haworth O, Cernadas M, Yang R, Serhan CN, Levy BD, Resolvin E1 regulates interleukin 23, interferon-gamma and lipoxin A4 to promote the resolution of allergic airway inflammation. Nat Immunol 9, 873–879 (2008). [PubMed: 18568027]
41. Chung KF, Wenzel SE, Brozek JL, Bush A, Castro M, Sterk PJ, Adcock IM, Bateman ED, Bel EH, Bleecker ER, Boulet LP, Brightling C, Chanez P, Dahlen SE, Djukanovic R, Frey U, Gaga M, Gibson P, Hamid Q, Jajour NN, Mauad T, Sorkness RL, Teague WG, International ERS/ATS guidelines on definition, evaluation and treatment of severe asthma. Eur Respir J 43, 343–373 (2014). [PubMed: 24337046]

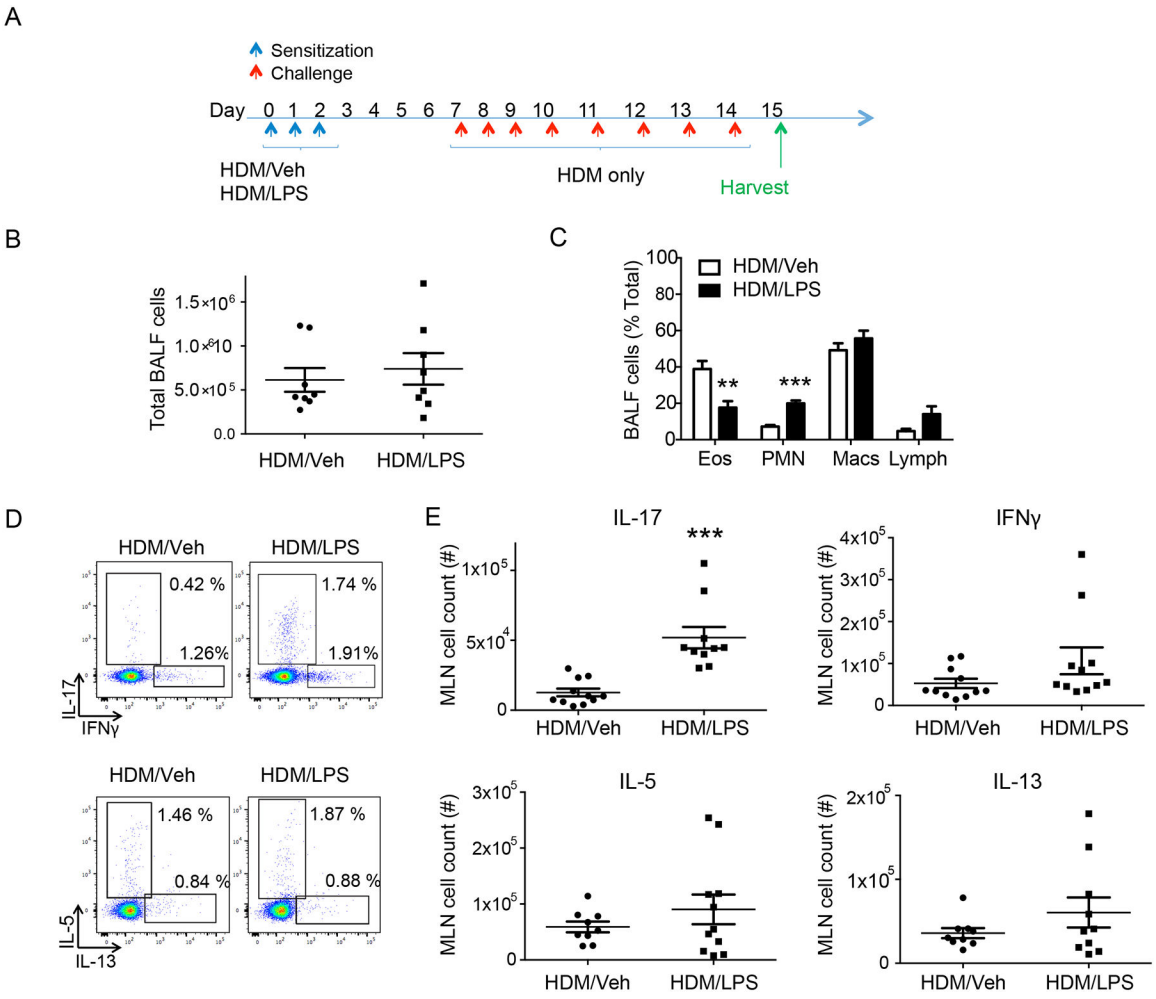

Figure 1: Neutrophilic inflammation in a murine model of HDM and LPS

(A) Schematic diagram showing the allergen sensitization and challenge protocol. After sensitization with HDM/Veh or HDM/LPS (protocol day 0–2) followed by HDM challenge (i.n., protocol day 7–14), the inflammatory response was assessed 24 hours later on protocol day 15 (n= 8 mice). (B) BALF total cell count (C) and leukocyte differential (% total leukocytes) were determined. (D,E) Mediastinal lymph nodes (MLN) were collected on protocol day 7 and dissociated cells were restimulated with PMA and ionomycin. (D) Representative flow cytometry plot and (E) MLN total cell count of CD4+ T cells expressing IL-17, IFN-γ, IL-5 and IL-13 (n = 10 mice). **P<0.01, ***P<0.001 by Student's t test

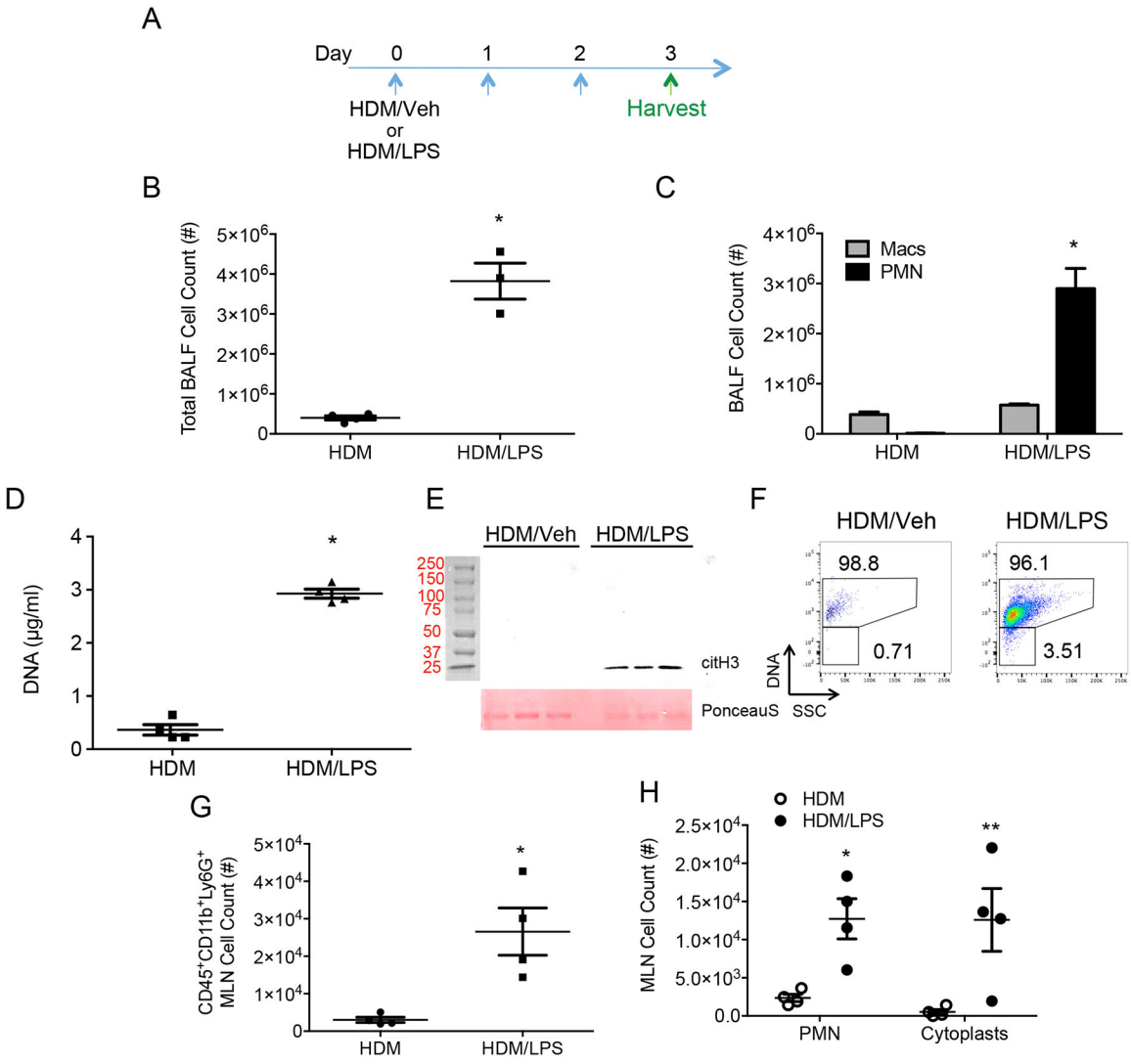

Figure 2: LPS promotes NETosis during allergen sensitization

(A) BAL fluid (BALF) and mediastinal lymph nodes (MLN) were harvested on protocol day 3 after allergen sensitization with HDM/Veh or HDM/LPS. (B) BALF total cell count and (C) leukocyte differential count on protocol day 3 from HDM/Veh or HDM/LPS sensitized mice. Data are representative of two independent experiments with n>3. (D) PicoGreen assay showing NET- associated DNA present in BALF (n = 4 mice). (E) A western blot showing hyper-citrullinated histone H3 in BALFs (top panel) and Ponceau S stain as loading control (bottom panel) (F) A representative flow cytometry plot showing the presence of DNA positive neutrophils (PMN) and DNA negative cytoplasts in BALFs from HDM/Veh (left) and HDM/LPS (right) mice (n = 8). (G) MLN total cell count for CD45+CD11b+Ly6g + cells and (H) DNA positive PMN and DNA negative cytoplast count (n = 4 mice). *p <0.05, **p < 0.01, ***p < 0.001 by two-tailed unpaired Student's t test where indicated or Mann Whitney U test.

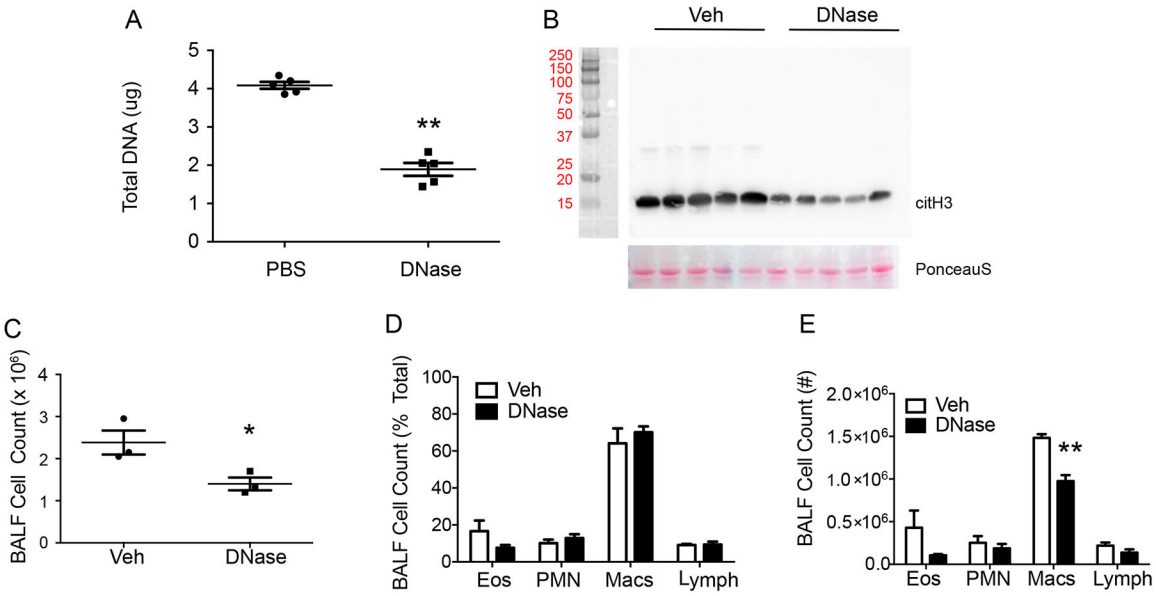

Figure 3: DNase instillation altered levels of NETs, but not neutrophilia

Mice were subjected to DNase (i.n., 6 hours post-sensitization with HDM/LPS) or PBS control and tissues were harvested at the end of the sensitization period (day 3). (A) Picogreen assays showing the amount of DNA in BALFs (n = 5 mice). (B) Western blot showing hyper- citrullinated histone H3 (top panel) and Ponceau S stain as loading control (bottom panel) (n = 5 mice). (C-E) To assess inflammatory responses, BAL was performed at the end of the allergen (HDM) challenge on protocol day 15. (C) BALF total cell count and (D, E) leukocyte differential (% total leukocytes and cell count) were enumerated (n = 3 mice). *P<0.05, **P<0.01 by Student's t-test.

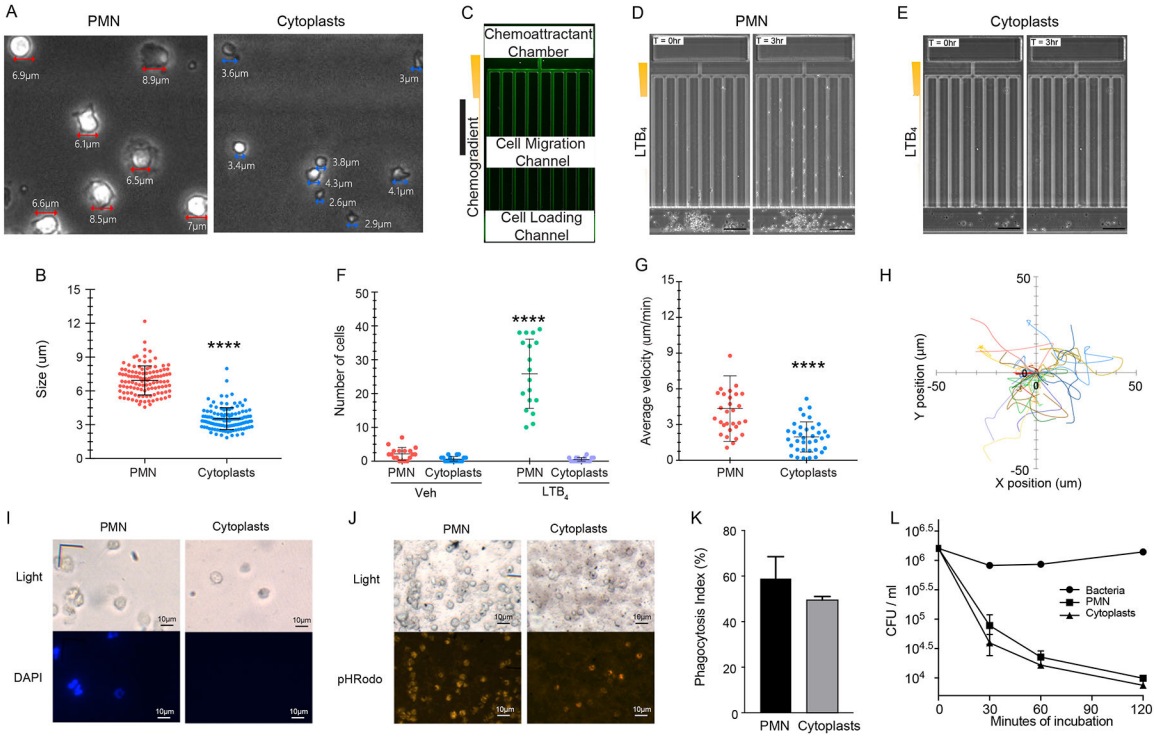

Figure 4: Enucleated cytoplasts formed after NETosis are intact and retain functional responses

Neutrophils (PMN) and neutrophil cytoplasts were flow sorted from HDM/LPS treated mouse lungs (protocol day 3). (A,B) The morphology and size of the sorted PMN and cytoplasts were determined by phase contrast microscopy. ****$p < 0.0001$ by two-tailed Student's t-test. (C-E) Chemotaxis to LTB4 was assessed using a microfluidics device with sorted cells (see Methods) (C) Fluorescent microscopic image showing one chemotaxis unit in the microfluidic device. (D) PMN or (E) cytoplasts were loaded into the microfluidics chamber with an LTB4 (100nm) gradient and time lapse, phase-contrast microscopic imaging was performed for 6 hours (Representative images). (F) Measurements of the number of cells that entered the migration microchannels per unit at various conditions. ****$p < 0.0001$ using a one-way ANOVA. (G) Measurements of chemotaxis velocity of PMN in the migration channels and chemokinesis velocity of cytoplasts in the cell loading channel ****$p < 0.0001$ using a one-way ANOVA. (H) Individual trajectories of cytoplast chemokinesis in the cell-loading channel. (I-K) Phagocytosis by PMN and cytoplasts was determined using pHRodo-coupled *E. coli* particles. (I) The absence of nuclei in cytoplasts confirmed by DAPI staining. (J) Phagocytosis of pHrodo-*E.coli* particles leading to fluorescent color change in PMN and cytoplasts. (K) Phagocytosis index (%Total) was determined. This experiment was performed 3 times. Values represent the mean and error bars SEM. (L) The killing capacity of sorted neutrophils and cytoplasts towards *Streptococcus pneumoniae* (serotype 1) was determined at different time points indicated. This experiment was performed 2 times. Values represent the mean between duplicate controls and error bars SEM used in a representative experiment.

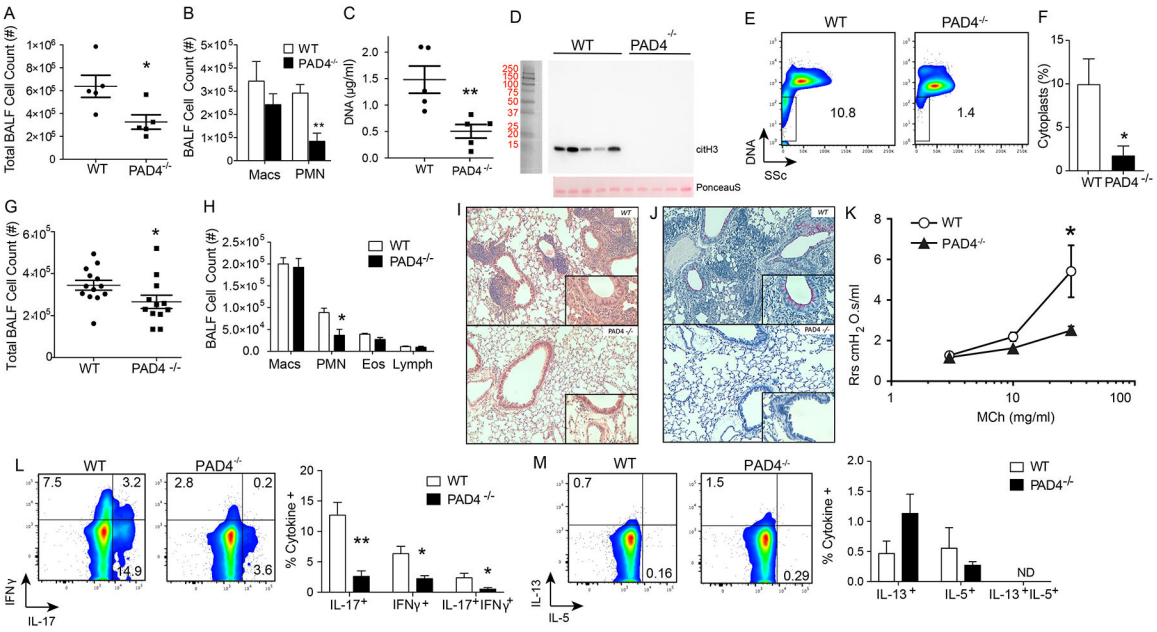

Figure 5: Deficiency in PAD4 results in decreased cytoplasts, neutrophils and IL-17

WT and PAD4−/− mice were sensitized with HDM/LPS and BALFs were collected on day 3. (A) BALF total cell count and (B) leukocyte differential were enumerated (n = 5 mice). (C) Netosis was monitored by BALF DNA levels on day 3 (n = 5 mice), and (D) Western blot for hyper- citrullinated histone H3 (top panel). Ponceau S stain was used as a loading control (bottom panel). (E) Representative flow cytometry plot showing DNA positive PMN and DNA negative cytoplasts in BALFs collected on protocol day 3 after HDM/LPS sensitization from WT and PAD4−/− mice. (F) Percent cytoplasts were enumerated by flow cytometry criteria. (G-K) In addition to the post-sensitization period, the resulting antigen-driven lung inflammation in WT and PAD4−/− mice was determined on protocol day 15 after HDM/LPS sensitization followed by HDM challenge. (G) BALF total cell count and (H) BALF differential count were measured. Lung histology between WT and PAD4−/− mice was evaluated by (I) H&E staining. (J) PAS staining. (K) AHR was measured in anesthetized mice that were mechanically ventilated in the presence of ascending doses of inhaled methacholine. (L) IL-17, and IFN-γ and (M) IL-13, and IL-5. Values represent the mean and error bars SEM (For M and N, error bars represent SD). *p < 0.05, **p < 0.01 using a Student's t-test.

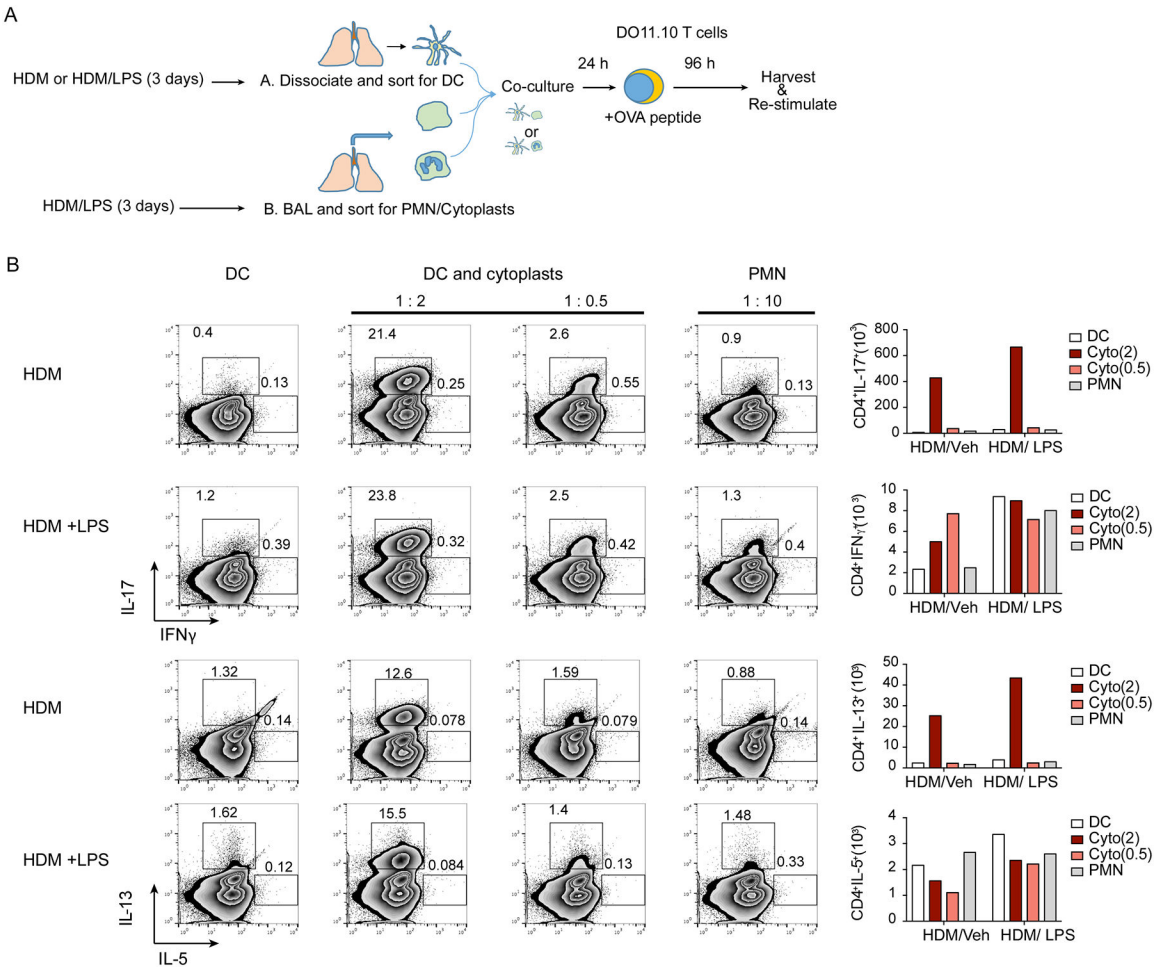

Figure 6: Lung cytoplasts interact with dendritic cells to induce antigen-specific Tlymphocytes.

(a) Schematic diagram showing the antigen-specific T cell activation protocol. Briefly, dendritic cells (DC) were harvested from the lungs of HDM/Veh or HDM/LPS sensitized mice and were incubated overnight with cytoplasts or neutrophils (PMN) at the indicated cell ratios (top of plots) of DC:cytoplasts (1:2 and 1:0.5) and DC:PMN (1:10). The HDM/Veh and HDM/LPS DCs were then co-cultured with naïve CD4+ T cells from DO11.10 mice in the presence of ovalbumin peptide and T cells were re-stimulated and stained for intracellular cytokines (see Methods). (b) Representative flow cytometry plots showing T cells expressing the indicated cytokines. Numbers outside the box represent % of CD4+ T cells. Bar graphs (right) show the absolute cell count for number of cells expressing the indicated cytokine. Data are representative of two experiments.

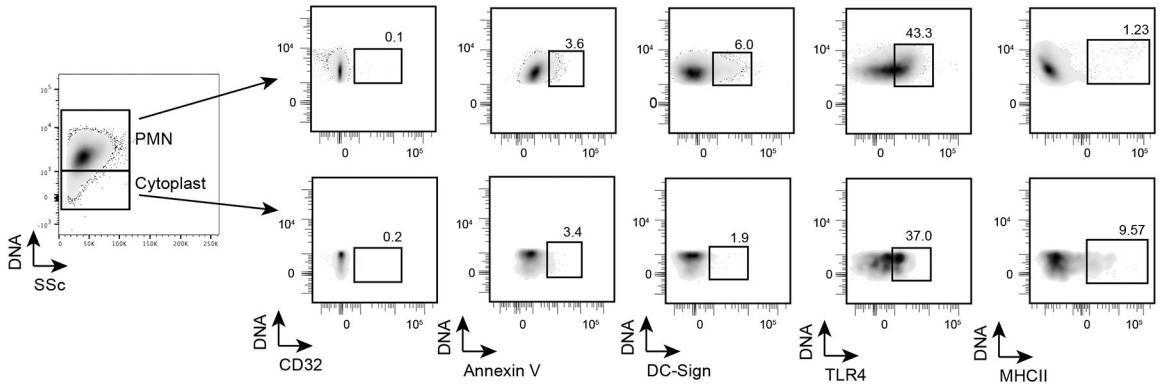

Figure 7: Select cytoplast surface proteins are distinct from intact neutrophils.

BALF from HDM/LPS sensitized mice were stained with different antibodies to detect the expression of these markers on neutrophils and cytoplasts. The expression of the markers is shown in the flow cytometry plots along with the percentage of positivity for each cell population. This experiment was performed twice.

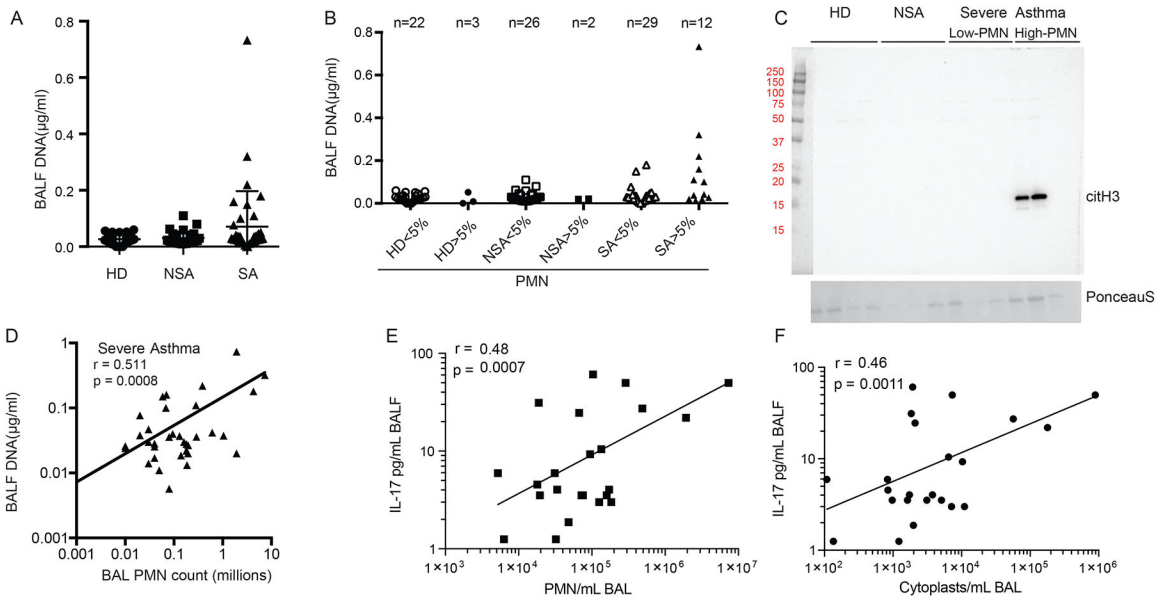

Figure 8: Lung NETosis in severe asthma correlates with BALF IL-17.

(A) Picogreen assays of BALF DNA in biospecimens from healthy donors (HD) and subjects with non-severe asthma (NSA) and severe asthma (SA). (B) BALF DNA levels were further stratified into low neutrophil (PMN) (< 5 %) and high PMN (> 5 %). (C) Representative western blot showing hyper-citrullinated histone H3 in BALFs from HD, NSA and SA with low or high PMN count (top panel) and Ponceau S stain as loading control (bottom panel). (D) Correlation between BALF DNA and PMN count in SA. (E) Correlation between BALF IL-17 levels and number of PMN (F) Correlation between BALF IL-17 levels and number of BALF cytoplasts. Pearson correlation r values and significance are noted for each correlation and regression lines are shown.